Location-Aware Point-to-Point RPL in Indoor IR-UWB Networks

Jiwon Jung, Yunyoung Choi and Younggoo Kwon *

Department of Electrical and Electronics Engineering, Konkuk University, Seoul 05029, Korea;
metri@naver.com (J.J.); dsung426@naver.com (Y.C.)
***** Correspondence: ygkwon@konkuk.ac.kr

check for updates

Abstract: Wireless multi-hop ad hoc routing is one of the critical design factors that determine the network performance of various wireless IoT applications. IETF has standardized the point-to-point RPL (P2P-RPL) routing protocol to overcome the inefficient routing overheads of RPL. However, P2P-RPL propagates the route discovery forwarding packets throughout the whole network. P2P-RPL suffers from the high energy consumption and the huge route discovery overhead in low-power and lossy networks (LLNs). In this paper, we propose a novel Location-Aware P2P-RPL (LA P2P-RPL), which achieves the energy-efficient P2P data delivery without reducing the networking reliability. The proposed algorithm introduces the Impulse-Response UWB (IR-UWB) based cooperative multi-hop self localization algorithm and the Location-Aware P2P-RPL algorithm for Indoor IR-UWB based networks. To increase the localization accuracy, smartphone based Inertial Navigation System (INS) with particle filtering is used in indoor multi-hop environments. The performance evaluations for Location-Aware P2P-RPL algorithm are compared with the traditional P2P-RPL and the ER-RPL algorithm to show the significant performance improvements for route discovery overheads and energy consumptions in LLNs.

Keywords: P2P-RPL; energy efficient routing; UWB multi-hop localization

1. Introduction

Wireless multi-hop ad hoc routing should provide the reliable interoperability in low-power and lossy networks (LLNs). The IETF standardized the IPv6 Routing Protocol for Low-Power and Lossy Networks (RPL) [1]. RPL constructs and maintains a tree-structured topology called Destination-Oriented Directed Acyclic Graphs (DODAG), and always forwards packets over pre-identified links to improve the energy efficiency of battery-dependent devices. The configuration of DODAG aims to minimize routing costs between the root and each node in the network. RPL is optimized for multipoint-to-point (MP2P) communication. RPL has adopted a tree-based proactive routing scheme for the low-power operation, and inherently suffers from the inefficiency of point-to-point (P2P) routing. When two non-root nodes need to communicate with each other, the packets must be passed upward until they reach a common ancestor that knows the path to the destination node. This simple routing strategy may result in long end-to-end delay and low packet delivery ratio due to significantly suboptimal P2P paths and heavy traffic congestion near the root. To compensate for these shortcomings, IETF standardized a new routing protocol, reactive discovery of point-to-point Routes in Low-Power and Lossy Networks (P2P-RPL) [1–4]. P2P-RPL constructs a temporary DAG that is solely for P2P route discovery to find efficient new paths to one or more nodes within the RPL framework. As a reactive routing protocol, P2P-RPL finds the best on-demand path in a lossy network. Since P2P-RPL is based on a broadcasting approach, it could lead to serious

medium contention known as the broadcast storm problem [4,5]. It is very important to achieve high reliability and consume less energy at the same time in P2P-RPL approaches.

IEEE 802.15 Working Group established a Impulse Radio Ultra WideBand (IR-UWB) based physical layer standard (IEEE802.15.4a) with precise ranging capability [6]. Impulse Radio Ultra-WideBand (IR-UWB) system has bandwidth wider than 500 MHz and uses narrow pulses to transmit and receive information. The short duration of UWB pulse enables the identification of multipath components at high resolution, that makes IR-UWB as promising technology for various highly accurate positioning applications [7]. In this paper, we introduce Location-Aware P2P-RPL (LA P2P-RPL), which achieves energy-efficient P2P data delivery without compromising reliability. The ranging capability offered by UWB can be exploited to build a network coordinate map, enabling the location-aware multi-hop routing in upper layer protocols [8–11]. Smartphone based Inertial Navigation System (INS) with particle filtering is used to increase the localization accuracy in indoor multi-hop networking environments. The LA P2P-RPL protocol uses knowledge of location to reduce the search space for the desired route discovery. Limiting the search space results in fewer route discovery messages, and this feature improves the route discovery overhead significantly especially when the distance between the source and the destination node is short. We first introduce the UWB-based cooperative multi-hop positioning algorithm for location-aware routing. Since the positional state of a node inevitably contains some degree of inaccuracy, we use the positioning algorithm that can infer the location error level of individual nodes to reflect the location uncertainty in the routing. Then, we demonstrate how to perform the energy-efficient point-to-point routing by using the estimated location knowledge of the individual node. The experiment results show the performance improvement of the Location-Aware P2P-RPL algorithm in multi-hop LLN environments. LA P2P-RPL algorithm is modified on the RPL framework, and compared with the existing solutions such as P2P-RPL and ER-RPL in terms of route discovery overhead, energy consumption, and reliability.

The remainder of this paper is organized as follows. We begin with Section 2 by stating related research works for P2P-RPL problems. The proposed algorithm is explained in Sections 3 and 4. The experimental results and performance evaluations are presented in Section 5. We conclude the paper in Section 6.

2. Related Works

The improvement of the route quality performance for RPL and P2P-RPL depends on the network topology for route discovery. The cost associated with the P2P-RPL route discovery is very costly in terms of energy consumption especially for LLNs, because all nodes in the network need to participate in the formation of temporary DODAGs during the route discovery.

The Lightweight On-demand Ad hoc Distance vector routing protocol, Next Generation (LOADng) is an ad hoc on-demand distance vector routing for LLNs [12]. LOADng supports P2P, point-to-multipoint (P2MP), and MP2P traffic patterns. LOADng disseminates the route discovery packets throughout the whole network like P2P-RPL. Geographic routing uses the location information of nodes to forward data packets with the greedy algorithm. A node chooses the closest node to the destination as the next hop to forward the data packets. Geographic routing shows the routing problem for the selection of the stable next hop in LLNs. Geographic routing has to exchange the one hop or even two hop neighbor table periodically to update the location information through the whole network. The cost is huge in terms of energy consumption for LLN environments [13]. Energy-Efficient Region-based Routing Protocol for Low-Power and Lossy Networks (ER-RPL) is designed to use the existing DODAG structure of RPL for the P2P route discovery [4]. Through the self-localization procedure, only a portion of nodes perform the route discovery packet forwarding. The region-based route discovery and region-to-region routing without route discovery procedure are introduced. A distributed self-regioning algorithm is proposed to estimate the region of each node. In ER-RPL, the estimated location accuracy severely depends on the network configurations, which may result in the routing performance degradation from the inaccurate location information. Chaudhari et al.

proposed Mobility-Aware Energy-Efficient Routing (MAEER) by using the position information of each node in the network [14]. MAEER provides mobility support and P2P route discovery with low energy consumption. The location information comes from the distributive self-regioning based on simple DV-hop algorithm. MAEER keeps track of location information of each node and provides DODAG Information Solicitation (DIS) and DODAG Information Object (DIO) managements. If the nodes are not distributed uniformly, DV-hop based localization scheme gives the inaccurate location information for each node. RPL routing for mobile low power wireless sensor networks using Corona mechanism (Co-RPL) is based on the Corona algorithm to estimate the location of each node [15]. DAG root sends DIO periodically without trickle timer for continuous configuration changes. The DIO transmission interval is controlled based on the speed of the nodes. RPL protocol can capture the frequent topology changes. Co-RPL suffers from the high power consumption and the large amount of control overhead due to the periodical broadcasting. Barcelo et al. proposed KP-RPL which exploits a positioning method based on the confidence regions defined by the mobile nodes in order to manage node mobility [16]. The standard Kalman filter predicts the position and enhances the accuracy. The standard Kalman filter is applied for the linear model, the non-linear trajectory of mobile nodes causes the inaccurate positioning results.

The direct path UWB signal attenuation due to obstacles reduces the possibility of direct path signal detection at the receiver, which degrades the accuracy of the flight time-based ranging method [11]. The failure of direct path signal detection significantly deteriorates the inter-node distance measurement performance in multilateration based positioning algorithms [17]. This problem is more serious in UWB devices, which have to follow the power spectral density (PSD) regulation to mitigate the interference problem with other narrowband systems. The cooperative positioning algorithms by using multiple nodes can improve the positioning accuracy problem caused by the channel environments [8,11,18,19]. The Inertial Navigation System (INS) provides a methodology for tracking the position, direction, and speed (direction and movement speed) of a mobile device by using motion sensors (accelerometers) and rotation sensors (gyroscopes). Related research experiments have shown that the combination of cooperative positioning and INS algorithms results in accurate mobile node tracking and network-wide positioning performance improvement [18,20–22].

To reduce the cost associated with the P2P-RPL route discovery overhead, we use the UWB-based cooperative multi-hop positioning with smartphone INS tracking by particle filtering for the exact self-localization of each node. From the accurate location information for each network node, Location-Aware P2P-RPL algorithm is proposed with limiting the route discovery packet forwarding region adaptively based on the location information of the source and the destination nodes.

3. UWB-Based Cooperative Multi-Hop Self Localization

In this section, the fully-distributed Bayesian cooperative multi-hop positioning method is proposed to support the location-aided routing in UWB-based WPANs. To attach a location error field to the routing message and announce the statistical characteristics of the location error to neighbors, each node must be able to estimate its own location error characteristics. We use the two-dimensional network scenario and assume that the exact initial locations of the anchor nodes are known. We consider that N wireless nodes are ad-hoc deployed in the area of $A(m^2)$. The N wireless nodes are composed of N_A anchor nodes and N_N non-anchor nodes, satisfying $N_A \ll N_N$. All anchor nodes are static, and there are N_M non-anchor mobile nodes in the network. The set of all anchor nodes and all non-anchor nodes in the network are denoted as $\Omega_a = \{\eta_j \mid j \in \{1, \cdots, N_a\}\}$ and $\Omega_n = \{\eta_j \mid j \in \{N_a + 1, \cdots, N\}\}$, respectively. The set of mobile non-anchor nodes is denoted by $\Omega_m = \{\eta_j \mid j \in \{N - N_m + 1, \cdots, N\}\}$.

Figure 1 gives the overview of the proposed UWB-based cooperative multi-hop positioning system. The positioning module combines the Bounding-box (B-box) algorithm with utilizing UWB-based ranging measurements and particle filter-based inertial navigation. Each node observes B-box information of neighboring nodes through UWB Transceiver. B-box information includes the

location state of adjacent nodes and the measured distance information to the adjacent node. The B-box state of a node is initialized or updated through the B-box algorithm [23]. The particle filter-based inertial navigation system tracks the movements of mobile nodes. Each mobile node maintains a set of particles in the particle filtering process. The particle weighting module adjusts the weight of the particles according to the surrounding B-box information. The mobile tracking module has rotation tracking, step detection, and step length estimation procedures. The location of each particle is updated by using the inertial sensor output sequences. Whenever the B-box state of each node is updated, the particle weighting module removes particles which are located outside the B-box area. The B-box state of the mobile node is determined by the smallest rectangle area which contains all the survived particles.
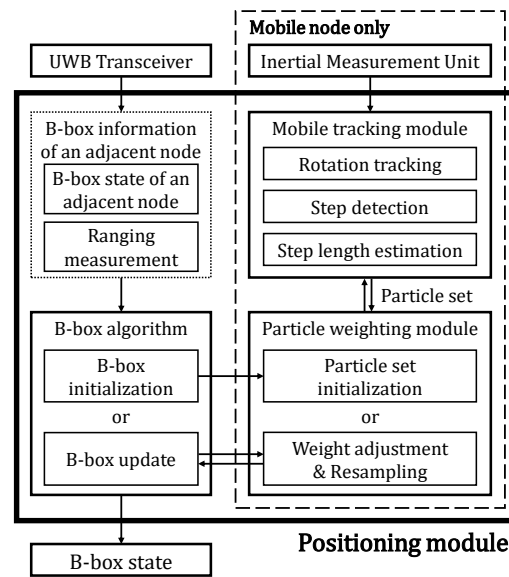

Figure 1. Ultra WideBand (UWB)-based cooperative multi-hop positioning.

3.1. UWB-Based Bounding-Box Multi-Hop Positioning

The B-box state, which represents a constraint on the actual position of a node, is defined as follows:

$$\mathbf{B}_j \equiv \begin{bmatrix} x_j^{lb} & x_j^{ub} & y_j^{lb} & y_j^{ub} \end{bmatrix}^T, \quad j = 1, \cdots, N \tag{1}$$

where $\mathbf{B}_j$ represents the B-box state of node η_j, *lb* and *ub* represent the lower and upper bounds on the position constraints. When the actual position coordinate of node η_j is $\left(x_j^a, y_j^a \right)$, the constraints of $x_j^{lb} \leq x_j^a \leq x_j^{ub}$ and $y_j^{lb} \leq y_j^a \leq y_j^{ub}$ must be satisfied.

For anchor nodes, the actual position coordinates are used as the B-box state as follows:

$$\mathbf{B}_j = \begin{bmatrix} x_j^a & x_j^a & y_j^a & y_j^a \end{bmatrix}^T, \quad \eta_j \in \Omega_a \tag{2}$$

Non-anchor nodes periodically update the B-box state by observing B-box information of nearby nodes. All nodes participating in the bounding-box algorithm recursively share B-box information with their neighbors. When a newly joined non-anchor node η_j observes B-box information of nearby node η_i, the information includes the B-box state of node η_i and the measured distance between the two nodes.

$$I_{ij,k} \equiv \left\langle \mathbf{B}_{i,k}, d_{ij,k} \right\rangle, \quad \eta_i \neq \eta_j \tag{3}$$

where $I_{ij,k}$ is the B-box information of node η_i observed by node η_j at the k th discrete time iteration, and $d_{ij,k}$ is the measured distance value between the two nodes. Observing $I_{ij,k}$, node η_j can initialize its B-box state as follows:

$$\mathbf{B}_{j,k} = \begin{bmatrix} x_{i,k}^{lb} - \left(d_{ij,k} + \delta \right) \\ x_{i,k}^{ub} + \left(d_{ij,k} + \delta \right) \\ y_{i,k}^{lb} - \left(d_{ij,k} + \delta \right) \\ y_{i,k}^{ub} + \left(d_{ij,k} + \delta \right) \end{bmatrix} \tag{4}$$

where δ is the absolute value of the worst negative-biased distance error that can occur in a UWB-based ranging process. In this paper, δ is set to 60 cm based on the ranging experiments with Decawave DW1000 modules [7]. The margin value δ prevents the B-box of nodes from becoming invalid due to ranging errors. Because the ranging error of the UWB system is typically biased on positive sides, it is possible to have a small margin value in the B-box algorithm [8,10,11,19]. If the B-box state of node η_j has already been initialized in the previous time slot, node η_j can update its B-box state using $I_{ij,k}$.

$$\mathbf{B}_{j,k} = \begin{bmatrix} max \left(x_{j,k-1}^{lb}, x_{i,k}^{lb} - \left(d_{ij,k} + \delta \right) \right) \\ min \left(x_{j,k-1}^{ub}, x_{i,k}^{ub} + \left(d_{ij,k} + \delta \right) \right) \\ max \left(y_{j,k-1}^{lb}, y_{i,k}^{lb} - \left(d_{ij,k} + \delta \right) \right) \\ min \left(y_{j,k-1}^{ub}, y_{i,k}^{ub} + \left(d_{ij,k} + \delta \right) \right) \end{bmatrix} \tag{5}$$

Figure 2 shows the process of determining the B-box state of non-anchor nodes. After the ranging session with anchor nodes, only some nodes near the anchors will have the initial B-box state. To broaden the positioning service coverage and gradually improve the positioning accuracy, it is necessary to perform additional B-box updates. As non-anchor nodes repeatedly share the initialized B-box state, more and more nodes can determine their B-box states through the network-wide B-box updates.
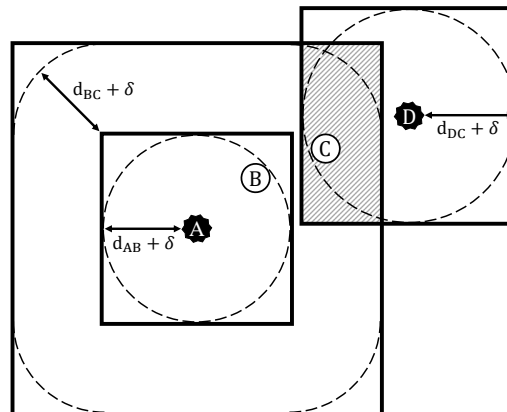

Figure 2. The process of determining the B-box state.

3.2. Mobile Node Tracking Based on the Inertial Navigation System with Particle Filtering

The Inertial Navigation System (INS) provides a methodology for tracking the position and the direction of a mobile device using inertial sensors. Particle filtering based INS is used to accurately track the B-box of the mobile node. The particle filter describes the posterior distribution of the probabilistic process, using a set of weighted samples. Every mobile node keeps one set of weighted particles to track its movement. Each particle has a state with the position and the orientation of the mobile node. The weight ω of each particle represents the probability of that particle being sampled. The state vector **s** of each particle consists of two-dimensional position coordinates **r** and the orientation

quaternion $\mathbf{q}$. Assuming that each mobile node holds N_p particles, the weighted particle set at node η_j is defined as:

$$\varsigma_{j,k} \equiv \left\{ \left\langle \mathbf{s}^l_{j,k}, \omega^l_{j,k} \right\rangle \mid l \in \{1, \cdots, N_p\} \right\}, \quad \eta_j \in \Omega_m \tag{6}$$

$$\begin{aligned} \mathbf{s}^l_{j,k} &\equiv \begin{bmatrix} \mathbf{r}^l_{j,k} & \mathbf{q}^l_{j,k} \end{bmatrix}^T \\ &= \begin{bmatrix} x^l_{j,k} & y^l_{j,k} & q^l_{0,j,k} & q^l_{1,j,k} & q^l_{2,j,k} & q^l_{3,j,k} \end{bmatrix}^T \end{aligned} \tag{7}$$

According to the particle set $\varsigma_{j,k}$, the posterior probability of the mobile node location is described as:

$$p\left(\mathbf{s}_{j,k}\right) \approx \sum_{l=1}^{N_p} \omega^l_{j,k} \delta\left(\mathbf{s}_{j,k} - \mathbf{s}^l_{j,k}\right) \tag{8}$$

where $\delta\left(\cdot\right)$ is the Dirac delta function. The particle filtering iteration of the mobile node begins with B-box initialization. At the beginning of the particle filtering, the positional state variable of each particle is sampled uniformly within the B-box region, and the orientation quaternions are initialized as arbitrary values in the entire state space because no relevant information is provided:

$$\varsigma_{j,k} \sim p\left(\mathbf{s}_{j,k} \mid \mathbf{B}_{j,k}\right), \quad \eta_j \in \Omega_m \tag{9}$$

If the particle set was initialized in the previous iteration, the weight of the particles is adjusted according to the state of the B-box state. Since all particles must be located in the B-box state, the weight of particles located outside the B-box area is adjusted to zero. The probability that each particle state of the mobile node satisfies the current B-box constraint is given by:

$$p\left(\mathbf{B}_{j,k} \mid \mathbf{s}^l_{j,k}\right) = \begin{cases} 1 & x^{lb}_{j,k} \le x^l_{j,k} \le x^{ub}_{j,k} \text{ and } y^{lb}_{j,k} \le y^l_{j,k} \le y^{ub}_{j,k} \\ 0 & else \end{cases} \tag{10}$$

Each particle state is associated with a weight. The adjusted weight is proportional to the probability that the particle follows the B-box constraint.

$$\omega^l_{j,k} \propto \omega^l_{j,k-1} p\left(\mathbf{B}_{j,k} \mid \mathbf{s}^l_{j,k}\right), \quad l = 1, \ldots, N_p \tag{11}$$

The particle states are independently updated according to the transition model to track the movement of the mobile node. In tracking of smartphones, the particle states are updated according to the pedestrian model, which includes step detection, step length estimation, and rotation tracking. Input sample values of the step length and heading direction are used to update the state of each particle. If no step event has been detected since the last prediction update, all step length values are set to zero. The step length values $\Delta\lambda$ are sampled according to the accelerometer and gyroscope output sequences $\boldsymbol{\alpha}_{0:k}, \boldsymbol{\gamma}_{0:k}$:

$$\left\{ \Delta\lambda^l_{j,k} \mid l \in \{1, \cdots, N_p\} \right\} \sim p\left(\Delta\lambda_{j,k} \mid \boldsymbol{\alpha}_{0:k}, \boldsymbol{\gamma}_{0:k}\right) \tag{12}$$

After sampling all the step length values, we need to determine the moving direction of each particle. Assuming that the frame relationship between the smartphone body and the pedestrian is fixed, we can use a smartphone inertial sensor to measure changes in the pedestrian moving direction. To get the current orientation quaternion state of each particle, we need to sample the rotation quaternion values $\Delta\mathbf{q}$ that represent the total angle the device has rotated since the last state update:

$$\left\{ \Delta\mathbf{q}^l_{j,k} \mid l \in \{1, \cdots, N_p\} \right\} \sim p\left(\Delta\mathbf{q}_{j,k} \mid \boldsymbol{\gamma}_{(k-1):k}\right) \tag{13}$$

Now all particles can update their position and orientation state vectors according to the sampled input values and the pedestrian motion model. The quaternion state of each particle is updated as follows:

$$\mathbf{q}_{j,k+1}^{l} = \Delta\mathbf{q}_{j,k}^{l} \otimes \mathbf{q}_{j,k}^{l}, \qquad l = 1, ..., N_p \tag{14}$$

where

$$\mathbf{q} \otimes \mathbf{q}' = \begin{bmatrix} q_0 & -q_1 & -q_2 & -q_3 \\ q_1 & q_0 & -q_3 & q_2 \\ q_2 & q_3 & q_0 & -q_1 \\ q_3 & -q_2 & q_1 & q_0 \end{bmatrix} \begin{bmatrix} q_0' \\ q_1' \\ q_2' \\ q_3' \end{bmatrix} \tag{15}$$

The orientation quaternion represents the 3D orientation. The orientation quaternion is used to calculate the 2D orientation that the mobile node is currently facing.

$$\psi_{j,k+1}^{l} = arctan \frac{2\left(q_{0,j,k+1}^{l} q_{3,j,k+1}^{l} + q_{1,j,k+1}^{l} q_{2,j,k+1}^{l}\right)}{1 - 2\left\{\left(q_{2,j,k+1}^{l}\right)^2 + \left(q_{3,j,k+1}^{l}\right)^2\right\}}, \qquad l = 1, ..., N_p \tag{16}$$

After sampling the moving distance and heading direction of each particle, the position state is updated as follows:

$$\mathbf{r}_{j,k+1}^{l} = \mathbf{r}_{j,k}^{l} + \Delta\lambda_{j,k}^{l} \begin{bmatrix} cos\left(\psi_{j,k+1}^{l}\right) \\ sin\left(\psi_{j,k+1}^{l}\right) \end{bmatrix}, \qquad l = 1, ..., N_p \tag{17}$$

After the movement tracking, the B-box state of the mobile node is determined as the smallest rectangle that contains all the survived particles, which is shown in Figure 3.
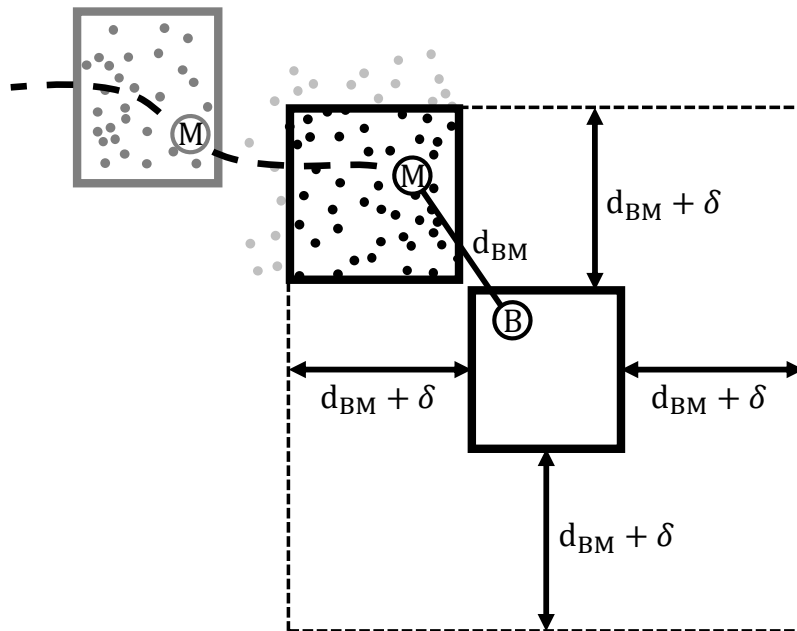

Figure 3. The process of adjusting weights in Particle Filtering.

After multiple iterations of the particle filtering process, the weights are concentrated on a small number of particles. We need to resample the set of particles to avoid the situation where the weight of a few particles dominate the rest of the samples. However, frequent resampling may cause the side effects such as sample impoverishment, so we need a criterion for implementing

resampling. The effective sample size (ESS) is a representative criterion when to perform the resampling procedure [24].

$$ESS_{j,k} = \left(\sum_{l=1}^{N_p} \left(\omega_{j,k}^l \right)^2 \right)^{-1} \tag{18}$$

Resampling is performed when the ESS is lower than the selected threshold τ_{ESS}. To avoid uncensored discarding of low-weighted particles, we use a method called deterministic resampling [25]. The deterministic resampling method keeps the original state density strictly, allowing particle filter to maintain sample diversity without sample impoverishment problems [26].

Figure 4 shows the CDF of the average estimated errors for the proposed cooperative multi-hop positioning algorithm. Decawave DW1000 device is used for distance measuring in physical radio channel. In basic simulation network configurations, 200 stationary nodes are randomly deployed in a 150 m × 150 m network area while anchor nodes are deployed at every 25 m, 50 m, 75 m, 100 m, 125 m, 150 m. Five mobile nodes are moving continuously with slow random walking speed and operate as leaf nodes without intermediate route forwarding features in route discovery procedures [27,28].
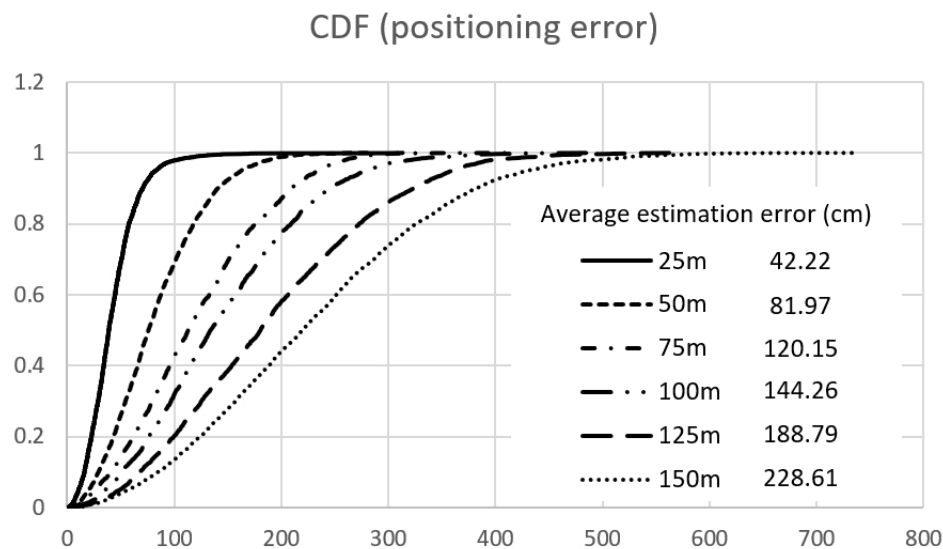

Figure 4. CDF for the proposed cooperative multi-hop positioning algorithm.

4. Location-Aware P2P-RPL for Indoor IR-UWB Based Network with Self Localization

The cost associated with the P2P route discovery is significantly high for LLNs, because all nodes in the network need to participate in the formation of temporary DODAGs during the route discovery. Based on the cooperative self-localization algorithm for indoor IEEE802.15.4a IR-UWB networks, we propose the Location-Aware P2P-RPL (LA P2P-RPL). LA P2P-RPL is a reactive P2P route discovery protocol that operates on RPL-based networks. In Location-Aware P2P-RPL, the temporary DAG is configured only within the routing request area, which is a rectangular region determined by the B-box state and the estimated location information of the source and destination nodes. Whenever a non-anchor node receives the location states of its neighboring nodes, the node updates its own location state. The state includes two-dimensional position information of the lower and upper bounds of the position estimates, respectively. The position information is piggybacked on the standard RPL control messages (DIO and DAO). To reduce the routing packet flooding overheads of P2P-RPL, the routing packet forwarding zone is determined by the estimated region of the source and the destination nodes. The four corners of the routing packet forwarding zone are determined based on the estimated position information of the source and destination nodes through self-localization procedure.

P2P-RPL forms a temporary DAG rooted at the origin solely for the P2P route discovery process. In P2P-RPL, the DODAG Information Object (DIO) acts as a route discovery message. A P2P mode

DIO carries exactly one P2P Route Discovery Option (P2P-RDO), which specifies the address for the target. When a router joins a temporary DAG advertised by a P2P mode DIO, it maintains its membership in the temporary DAG for the duration indicated by the L field inside the P2P-RDO. When a target node receives a P2P mode DIO, the P2P-RDO contains a complete source route from the origin to this target. The links in the discovered route have bidirectional reachability, and the target replies a P2P Discovery Reply Object (P2P-DRO) to the source through the discovered route. On receiving a P2P-DRO message, the origin stores the discovered route in its memory. The connection setup procedure of Location Aware P2P-RPL is shown in Figure 5. When a connection request is generated, the origin measures the cost of reaching the target by sending a measurement object (MO) along the pre-established global DAG. On receiving a Measurement Request, an intermediate router updates the routing metric values inside the message and forwards it to the next hop on the route. When the target receives the MO and the routing cost (ETX) is satisfied within the threshold value, it sends a measurement reply back to the origin to inform the cost of the route. In LA P2P-RPL, the measurement reply also carries the B-box state of the target with the location option. If the origin fails to receive the corresponding Measurement Reply, the origin does not know the position of the target, and inevitably starts route discovery according to P2P-RPL. If the routing cost is not satisfied for the current routing path constraints, the target node initiates the LA P2P-RPL route discovery in the limited route forwarding request area based on the estimated location information of the origin node and the target node.
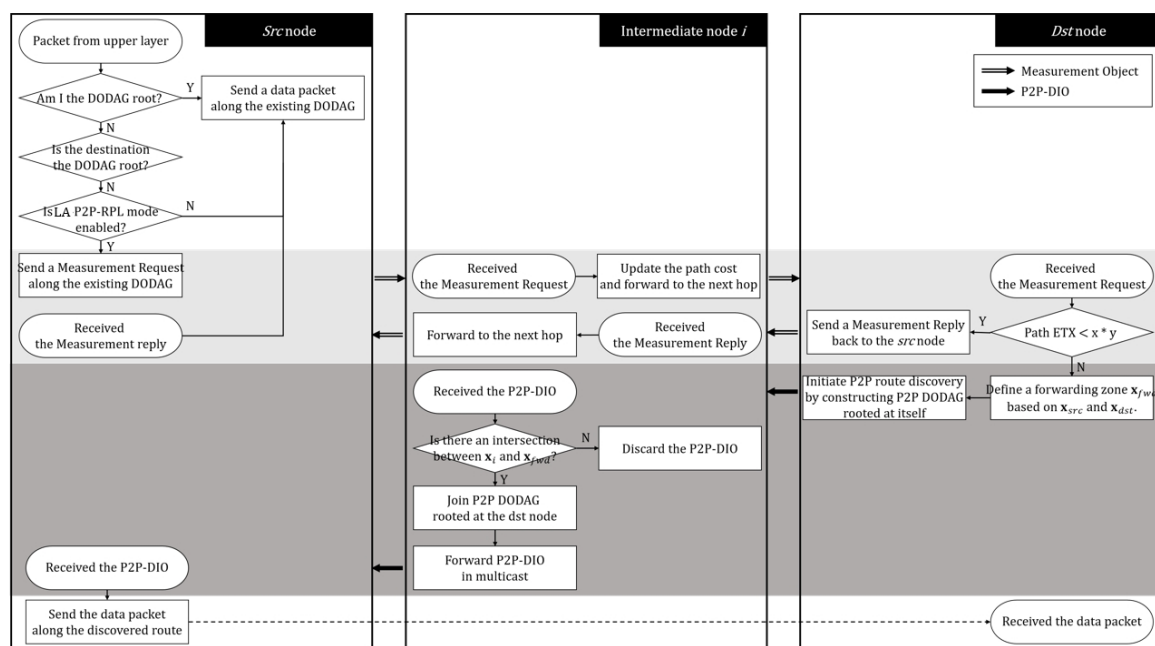

Figure 5. The flow chart of Forwarding Zone based point-to-point (P2P) route discovery.

The determined request area is piggybacked into the P2P mode DIO in the form of a location option. An intermediate router receiving a P2P mode DIO with the location option checks whether its B-box overlaps the request area. A router, including the target, discards the received P2P mode DIO if its B-box does not overlap with the request area. This positional constraint is used to limit the propagation of P2P mode DIO messages.

LA P2P-RPL has a limited propagation area for route discovery messages. If a route is not discovered within a timeout period, LA P2P-RPL initiate a new route discovery with the P2P-RPL algorithm. Note that the probability of finding a path (in the first attempt) can be increased by enlarging the size of the initial route forwarding request area. However, the route discovery overhead

also increases with the size of the request area. There is a trade-off between the latency of route determination and the message overhead.

Location-Aware P2P Route Discovery Forwarding Zone

As the results of self-localization are obtained, all nodes have their own up-to-date position state. LA P2P-RPL defines the route discovery packet forwarding zone based on the position states of the source and destination nodes. If the estimated region of a node belongs to the route discovery forwarding zone, the node forwards a P2P route discovery packet to its neighbor nodes. The operation for LA P2P-RPL route discovery forwarding zone is shown in Figure 6.
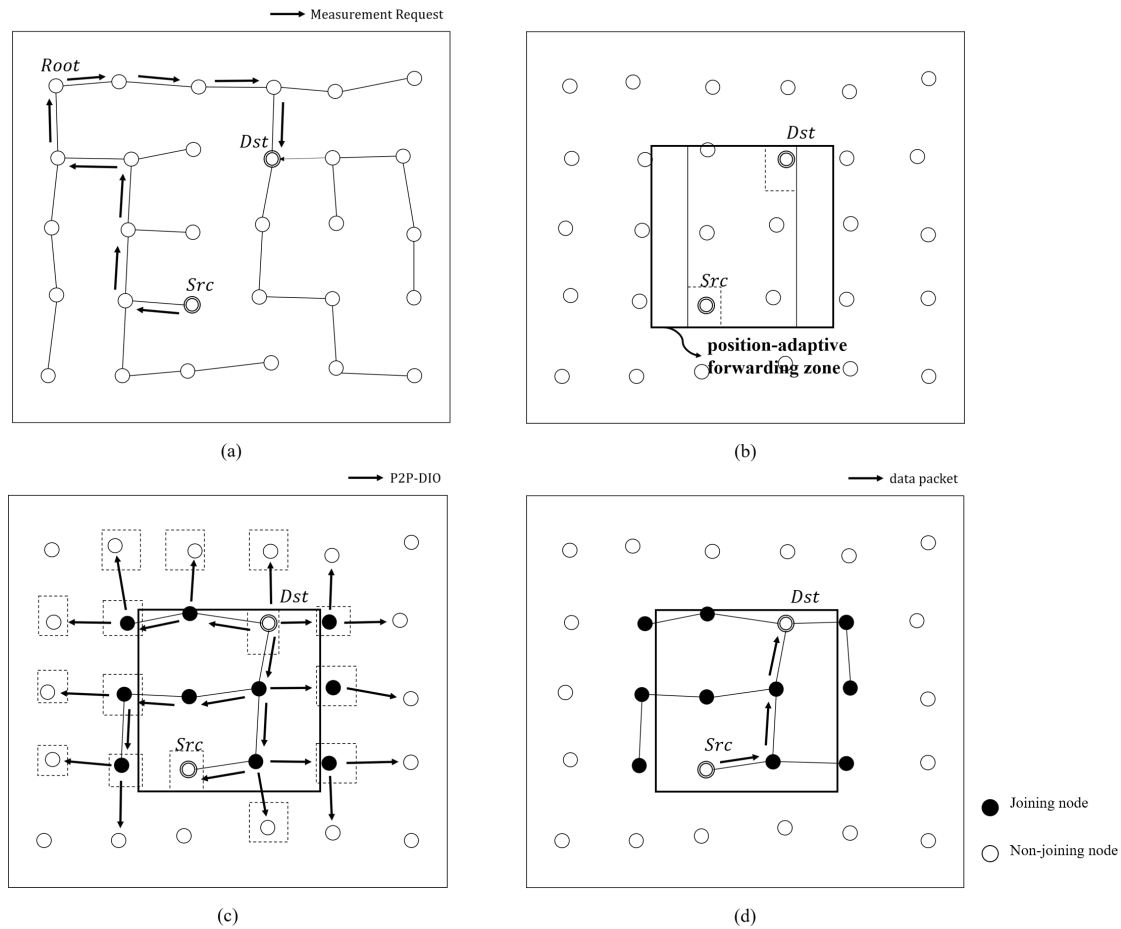
Figure 6. The operation for Route Discovery Packet Forwarding Zone of Location-Aware (LA) P2P-RPL (**a**) Measurement request procedure (**b**) Forwarding zone determination (**c**) Route discovery packet forwarding (**d**) Data transmission.

Assume that the source node (Src) tries to find the P2P route path to the destination node (Dst). In Figure 6a, the Src sends the measurement request which includes its position state to the Dst along the existing DAG. Upon receiving the measurement request, the Dst checks whether the accumulated path cost inside the request message satisfies the constraints or not. If the cost is not satisfied to the constraints, the Dst initiates the LA P2P-RPL route discovery. As shown in Figure 6b, the Dst defines the forwarding zone for P2P route discovery as the rectangular region that includes the current estimated position states of the Src and Dst nodes. We denote the forwarding zone position state $\mathbf{x}_{fwd}$ as follows.

$$\mathbf{x}_{fwd} = \begin{bmatrix} x_{lb,fwd} \\ x_{ub,fwd} \\ y_{lb,fwd} \\ y_{ub,fwd} \end{bmatrix} = \begin{bmatrix} min(x_{lb,s}, x_{lb,d}) \\ max(x_{ub,s}, x_{ub,d}) \\ min(y_{lb,s}, y_{lb,d}) \\ max(y_{ub,s}, y_{ub,d}) \end{bmatrix} \tag{19}$$

where *lb*, *ub*, *s*, *d* denotes low bound, upper bound, source, destination, respectively.

Then, the Dst node initiates the route discovery by constructing a temporary DODAG rooted at itself. Since the P2P path between the Src and the Dst is required over asymmetric links and RPL routes are optimized for upward routing, we set the Dst node as the root to improve the end-to-end delivery in LLNs. Before disseminating a P2P-DIO message, the Dst node piggybacks $\mathbf{x}_{fwd}$ on the message. Upon receiving P2P-DIO from its neighbor node, the intermediate node follows the procedure which is described in Figure 5. The node joins P2P route discovery only if there is an intersection between its estimated region and the forwarding zone. In Figure 6c, if the nodes that are not belong to the route discovery forwarding zone receive the P2P-DIO packet from the neighbor node, they simply discard the forwarding packet. Consequently, only small number of nodes which belong to the route discovery forwarding zone participate in the route discovery process, which reduces the network-wide route discovery packet flooding significantly. Once the Src node receives the P2P mode DIO message, the P2P path is established as the upward route to the root (Dst) of the temporary DODAG from the Src node as shown in Figure 6d. Then, the Src node sends the data packet along the discovered route to the Dst node.

5. Performance Evaluation

In this section, P2P-RPL, ER-RPL, and LA P2P-RPL are implemented on Cooja network simulator for Contiki operating system platform [29,30]. LA P2P-RPL implementation is based on the modules of ContikiRPL library and P2P-RPL implementation on Contiki platform. The software architecture of Location-Aware P2P-RPL is shown in Figure 7.
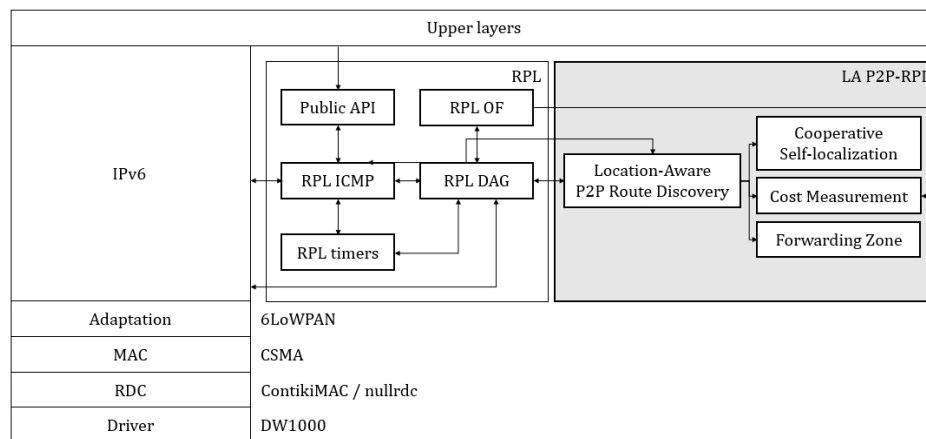

Figure 7. The software architecture of position-adaptive forwarding zone based P2P-RPL on Contiki OS.

The radio channel features are based on Decawave DW1000 UWB device radio characteristics on the lossy environments, and the simulation studies are conducted with the IEEE 802.15.4 [29,30]. In this paper, the network configuration is basically stationary for routing procedures just like in RPL and P2P-RPL operations. In basic simulation network configurations, 200 stationary nodes are randomly deployed in a 150 m × 150 m network area while anchor nodes are deployed at every 75 m, and the average estimated localization error is 120 cm. Five mobile nodes are moving continuously with slow random walking speed and operate as leaf nodes without intermediate route forwarding features in route discovery procedures [27,28]. In this simulation study, the source and the destination node pair is randomly selected for each traffic flow. We used the model of UWB frame transmission time and

the parameter setting validated by Charlier et al. in the testbed experiments [31,32]. The latency from initiating P2P route discovery by sending a P2P-DIO of 66 bytes to receiving the first P2P-DRO of 38 bytes takes much less than 1 s, which includes UWB packet transmission time and the time required for the P2P-DIOs to reach the destination node considering Trickle parameters. Other parameters are displayed in Table 1. A different random topology is generated and each data result is the average value from all simulation runs.

Table 1. Simulation parameters.

Parameter	Value
Radio environment	UDGM with distance loss
Transmission range	20
TX ratio (%)	99
RX ratio (%)	97
RPL mode of operation	Storing mode
Objective Function	MRHOF
Routing Metric	ETX
I_{min}	64 ms
I_{max}	256 ms
DIO redundancy (k)	1
Transmitter electronics ($E_{TX\text{-}elec}$)	33.97 nJ/bit
Transmitter amplifier (ϵ_{amp})	6 pJ/bit/m^2
Receiver electronics ($E_{RX\text{-}elec}$)	14.56 nJ/bit

The following metrics are adopted to evaluate the performance of the proposed protocol.

1. Routing control overhead refers to the total number of control messages for finding P2P routing path between the source node and the destination node.
2. Energy consumption refers to the total energy consumption for finding P2P routing path between the source node and the destination node. We only consider the energy consumption in transmitting and receiving states by using the first order radio model [33]. The parameters used in the first order radio model are shown in Table 1.
3. Average routing path finding success rate refers to the ratio of the successfully routing path finding number to the total number of the routing path finding attempts.
4. Average hop count refers to the average discovered P2P routing path hop length between the source node and the destination node.
5. Packet delivery ratio (PDR) refers to the ratio of the successfully received packet number on the destination node to the total generated packet number by the source node.

Figures 8–10 show the performance results for the network configuration of 150 m × 150 m with 200 nodes. Figure 8 shows that the routing control overhead for route discovery increases as the distance between the source node and the destination node increases. Even in the short range networking situations for P2P-RPL route discovery procedure, the route discovery forwarding packets are flooded through the whole network. Location-aware P2P-RPL reduces the unnecessary forwarding packets by using the location information of the source and the destination node. In LA P2P-RPL, if the distance between the source and the destination node is short, the route discovery forwarding zone is limited to a small area, which reduces the number of route discovery forwarding packets significantly. Figure 8 shows that LA P2P-RPL reduces the route discovery forwarding overhead significantly in short distance range. As the distance between the source and the destination node is increased, the route discovery forwarding zone of LA P2P-RPL is increased close to the whole network size of 150 m × 150 m, which results in increasing the route discovery forwarding overhead gradually close to P2P-RPL. LA P2P-RPL efficiently limits the route discovery forwarding zone with accurate self localization information, which improves the routing control overhead performance compared to ER-RPL too.
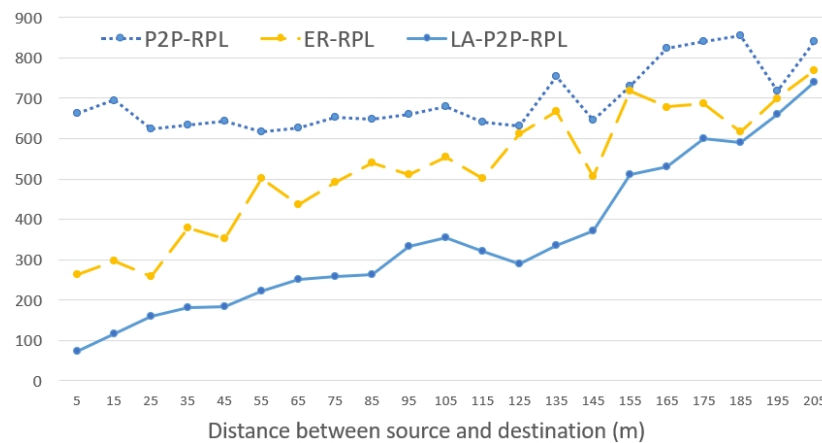
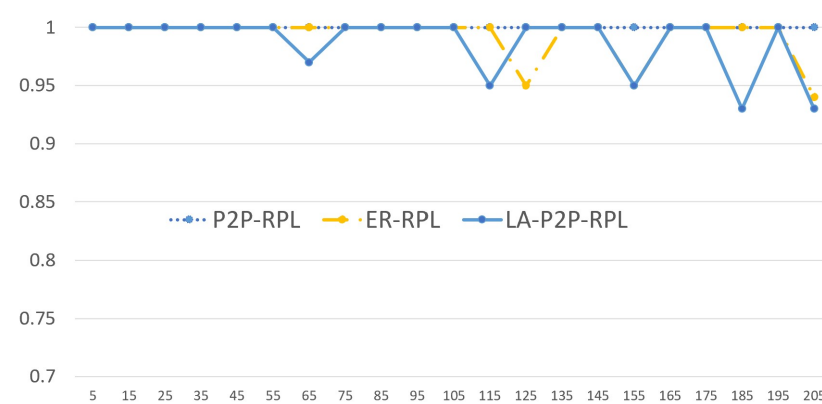**Figure 8.** Number of control message overhead.

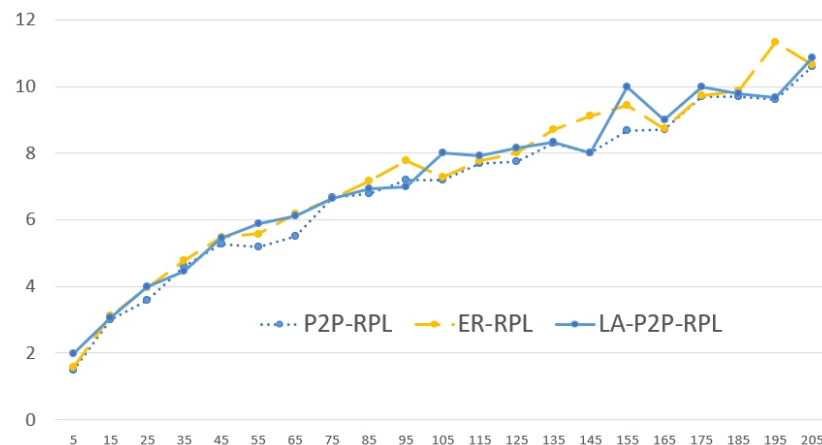**Figure 9.** Routing path finding success rate.

Figure 10. Average hop count.

Figure 9 shows that the routing path finding success rate of P2P-RPL, ER-RPL, and LA P2P-RPL. Since P2P-RPL searches the optimal route path by forwarding route discovery packets through the whole network, the proposed LA P2P-RPL with limited route discovery forwarding zone can not improve the routing path finding success rate performance better than P2P-RPL. However, Figure 9 shows that the routing path finding success rate performance of LA P2P-RPL is not degraded much compared with P2P-RPL in the self localization support network configurations of less than 10 m node displacement distance. As the distance between the source and the destination node increases, LA

P2P-RPL and ER-RPL can fail to find the routing path successfully around 5% while P2P-RPL shows the routing path finding success rate is close to 1.

Figure 10 shows that the average hop count of P2P-RPL, ER-RPL, and LA P2P-RPL. P2P-RPL can find the optimal (the smallest hop count) route path by forwarding the route discovery packets through the whole network. The proposed LA P2P-RPL can not find better route path (smaller hop count route path) than P2P-RPL, because LA P2P-RPL only searches the limited route discovery forwarding zone based on the source and the destination node location information. Figure 10 shows that the average hop count performance of LA P2P-RPL is degraded 2∼3% in short distance region of less than 45 m, and 4%∼6% in long distance region compared with P2P-RPL.

Figures 11–13 show the overall performance results for the network size variations of 75 m × 75 m, 150 m × 75 m, and 150 m × 150 m. The node density is the same for all simulations of 150 m × 150 m with 200 nodes at every 75 m anchor node configuration. Figure 11 shows the number of routing control message overhead to the network size variations. The routing control overhead increases as the network size increases. In the network size of 75 m × 75 m case, the performance difference is small among P2P-RPL, ER-RPL, and LA P2P-RPL. In the network size of 150 m × 150 m case, the routing control message overhead of LA P2P-RPL is significantly reduced compared to P2P-RPL and ER-RPL. The routing packet forwarding zone of LA P2P-RPL is reduced efficiently for route discovery procedure, which is come from the accurate self localization information of LA P2P-RPL compared with ER-RPL localization performance. LA P2P-RPL defines the routing forwarding zone depending on the location of the source and destination nodes to restrict the unnecessary flooding of DIO control messages. LA P2P-RPL achieves more than 50% control overhead performance improvements compared with P2P-RPL, and more than 30% control overhead performance improvements compared with ER-RPL.
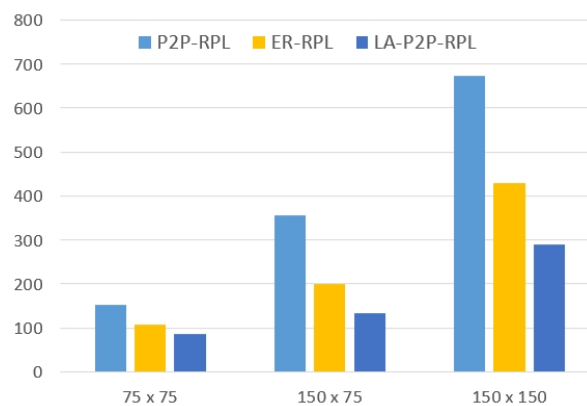

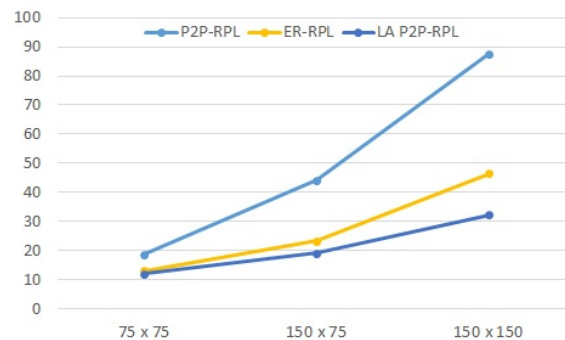**Figure 11.** Number of control message overhead vs. network size.

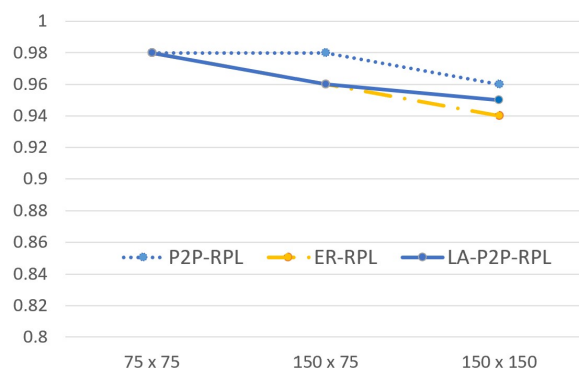**Figure 12.** Energy consumption [mJ] vs. network size.

Figure 13. Packet delivery ratio (PDR) vs. network size.

In Figure 12, LA P2P-RPL reduces around 50% and 10% total energy consumption in comparison with P2P-RPL and ER-RPL, respectively. In LA P2P-RPL, a node re-broadcasts a P2P-DIO message only if it is located in the route discovery forwarding zone. This reduces the number of P2P-DIO messages both in transmitting and receiving states. The energy model considers the energy consumptions for transmitting and receiving states, and the energy for sensing and processing data is not considered. The energy performance difference is increased significantly as the network size increases.

As shown in Figure 13, LA P2P-RPL achieves a very close performance results to ER-RPL and P2P-RPL for packet delivery ratio with symmetric physical links. Though partial nodes are involved in route discovery process, ER-RPL, and LA P2P-RPL can provide reliable routing path. In LA P2P-RPL, the temporary DODAG is rooted at the destination node, which can handle the route discovery under asymmetric links with low PDR performance degradation.

6. Conclusions

In this paper, the Location-Aware P2P-RPL (LA P2P-RPL) algorithm is proposed, which introduces the Impulse-Response UWB (IR-UWB) based cooperative multi-hop self localization algorithm and the Location-Aware P2P-RPL algorithm for Indoor IR-UWB based networks. Smartphone based Inertial Navigation System (INS) with particle filtering is combined with B-box algorithm to improve the localization accuracy in indoor multi-hop UWB networking environments. The proposed algorithm achieves the energy-efficient P2P data delivery without reducing the networking reliability, and reduces the route discovery message overheads significantly especially in short distance P2P routing operations. Experimental results show that the proposed LA P2P-RPL works effectively to reduce the route discovery forwarding packets by limiting the route discovery region based on the accurate location information of the source and the destination nodes. As the network size increases, the proposed LA P2P-RPL saves the energy consumptions significantly by reducing the re-broadcasting P2P-DIO messages both in transmitting and receiving states compared with P2P-RPL and ER-RPL algorithms. LA P2P-RPL shows similar performance results for the route path finding success rate and the average hop count compared with P2P-RPL which forwards the route discovery packets throughout the whole network. In future research for LA P2P-RPL algorithm, the node mobility, the 3D self localization and 3D routing expansion, and the impacts of self localization errors in multi-hop UWB based networking environments are being prepared.

Author Contributions: J.J. and Y.K. contributed to the main idea of this research. J.J. and Y.C. performed the implementations and simulations. All authors contributed to the writing of this paper. All authors have read and agreed to the published version of the manuscript.

References

1. Zhao, M.; Kumar, A.; Chong, P.; Lu, R. A comprehensive study of RPL and P2P-RPL routing protocols: Implementation, challenges and opportunities. *Peer-to-Peer Netw. Appl.* **2017**, *10*, 1232–1256. [CrossRef]
2. Baccelli, E.; Philipp, M.; Goyal, M. The P2P-RPL routing protocol for IPv6 sensor networks: Testbed experiments. In Proceedings of the SoftCOM 2011, 19th International Conference on Software, Telecommunications and Computer Networks, Split, Croatia, 15–17 September 2011; pp. 1–6.
3. Goyal, M.; Baccelli, E.; Philipp, M.; Brandt, A.; Martocci, J. *Reactive Discovery of Point-to-Point Routes in Low-Power and Lossy Networks*; RFC 6997; IETF Working Groups: Fremont, CA, USA, 2013.
4. Zhao, M.; Ho, I.; Chong, P. An Energy-Efficient Region-Based RPL Routing Protocol for Low-Power and Lossy Networks. *IEEE Internet Things J.* **2016**, *3*, 1319–1333. [CrossRef]
5. Tseng, Y.C.; Ni, S.Y.; Chen, Y.S.; Sheu, J.P. The broadcast storm problem in a mobile ad hoc network. *Wirel. Netw.* **2002**, *8*, 153–167. [CrossRef]
6. *IEEE Standard for Information Technology—Local and Metropolitan Area Networks—Specific Requirements—Part 15.4: Wireless Medium Access Control (MAC) and Physical Layer (PHY) Specifications for LowRate Wireless Personal Area Networks (WPANs): Amendment 1: Add Alternate PHYs*; IEEE Standard 802.15.4a-2007; IEEE Standards Association: Piscataway, NJ, USA, 2007.
7. Ruiz, A.R.J.; Granja, F.S. Comparing ubisense, bespoon, and decawave uwb location systems: Indoor performance analysis. *IEEE Trans. Instrum. Meas.* **2017**, *66*, 2106–2117. [CrossRef]
8. Wymeersch, H.; Lien, J.; Win, M. Cooperative Localization in Wireless Networks. *Proc. IEEE* **2009**, *97*, 427–450. [CrossRef]
9. Galstyan, A.; Krishnamachari, B.; Lerman, K.; Pattem, S. Distributed Online Localization in Sensor Networks Using a Moving Target. In Proceedings of the 3rd International Symposium on Information Processing in Sensor Networks, Berkeley, CA, USA, 26–27 April 2004; pp. 61–70.
10. Ismail, G.; Chong, C. A Survey on TOA Based Wireless Localization and NLOS Mitigation Techniques. *IEEE Commun. Surv. Tutor.* **2009**, *11*, 107–124.
11. Dardari, D.; Conti, A.; Lien, J.; Win, Z. The Effect of Cooperation on UWB-Based Positioning Systems Using Experimental Data. *EURASIP J. Adv. Signal Process.* **2008**, 513873. [CrossRef]
12. Sobral, J.V.; Rodrigues, J.J.; Rabêlo, R.A.; Saleem, K.; Furtado, V. LOADng-IoT: An enhanced routing protocol for internet of things applications over low power networks. *Sensors* **2019**, *19*, 150. [CrossRef] [PubMed]
13. Adnan, A.I.; Hanapi, Z.M.; Othman, M.; Zukarnain, Z.A. A Secure Region-Based Geographic Routing Protocol (SRBGR) for Wireless Sensor Networks. *PLoS ONE* **2017**, *12*, e0170273. [CrossRef] [PubMed]
14. Chaudhari, S.S.; Maurya, S.; Jain, V.K. MAEER: Mobility aware energy efficient routing protocol for Internet of Things. In Proceedings of the 2017 Conference on Information and Communication Technology (CICT), Gwalior, India, 3–5 November 2017; pp. 1–6.
15. Gaddour, O.; Koubâa, A.; Rangarajan, R.; Cheikhrouhou, O.; Tovar, E.; Abid, M. Co-RPL: RPL routing for mobile low power wireless sensor networks using Corona mechanism. In Proceedings of the 9th IEEE International Symposium on Industrial Embedded Systems (SIES 2014), Pisa, Italy, 18–20 June 2014; pp. 200–209.
16. Barcelo, M.; Correa, A.; Vicario, J.L.; Morell, A.; Vilajosana, X. Addressing mobility in RPL with position assisted metrics. *IEEE Sens. J.* **2015**, *16*, 2151–2161. [CrossRef]
17. Alarifi, A.; Al-Salman, A.; Alsaleh, M.; Alnafessah, A.; Al-Hadhrami, S.; Al-Ammar, M.A.; Al-Khalifa, H. Ultra wideband indoor positioning technologies: Analysis and recent advances. *Sensors* **2016**, *16*, 707. [CrossRef] [PubMed]
18. Liu, R.; Yuen, C.; Do, T.N.; Zhang, M.; Guan, Y.L.; Tan, U.X. Cooperative positioning for emergency responders using self IMU and peer-to-peer radios measurements. *Inf. Fusion* **2020**, *56*, 93–102. [CrossRef]
19. Alsindi, N.; Pahlavan, K. Cooperative localization bounds for indoor ultra-wideband wireless sensor networks. *EURASIP J. Adv. Signal Process.* **2007**, *2008*, 852509. [CrossRef]
20. Wang, J.; Gao, Y.; Li, Z.; Meng, X.; Hancock, C.M. A tightly-coupled GPS/INS/UWB cooperative positioning sensors system supported by V2I communication. *Sensors* **2016**, *16*, 944. [CrossRef] [PubMed]
21. Liu, R.; Yuen, C.; Do, T.N.; Jiao, D.; Liu, X.; Tan, U.X. Cooperative relative positioning of mobile users by fusing IMU inertial and UWB ranging information. In Proceedings of the 2017 IEEE International Conference on Robotics and Automation (ICRA), Singapore, 29 May–3 June 2017; pp. 5623–5629.

22. Seco, F.; Jiménez, A.R. Smartphone-based cooperative indoor localization with RFID technology. *Sensors* **2018**, *18*, 266. [CrossRef] [PubMed]

23. Simic, S.N.; Sastry, S. *Distributed Localization in Wireless Ad Hoc Networks*; Technical Report UCB/ERL; EECS UC BERKELEY: Berkeley, CA, USA, 2002; Volume 2, pp. 1–13.

24. Kong, A.; Liu, J.S.; Wong, W.H. Sequential imputations and Bayesian missing data problems. *J. Am. Stat. Assoc.* **1994**, *89*, 278–288. [CrossRef]

25. Li, T.; Sattar, T.P.; Sun, S. Deterministic resampling: Unbiased sampling to avoid sample impoverishment in particle filters. *Signal Process.* **2012**, *92*, 1637–1645. [CrossRef]

26. Li, T.; Bolic, M.; Djuric, P.M. Resampling methods for particle filtering: classification, implementation, and strategies. *IEEE Signal Process. Mag.* **2015**, *32*, 70–86. [CrossRef]

27. El Korbi, I.; Brahim, M.B.; Adjih, C.; Saidane, L.A. Mobility enhanced RPL for wireless sensor networks. In Proceedings of the 2012 Third International Conference on the Network of the Future (NOF), Gammarth, Tunisie, 21–23 November 2012; pp. 1–8.

28. Cobarzan, C.; Montavont, J.; Noel, T. Analysis and performance evaluation of RPL under mobility. In Proceedings of the 2014 IEEE Symposium on Computers and Communications (ISCC), Funchal, Portugal, 23–26 June 2014; pp. 1–6.

29. Dunkels, A.; Gronvall, B.; Voigt, T. Contiki-a lightweight and flexible operating system for tiny networked sensors. In Proceedings of the 29th Annual IEEE International Conference on Local Computer Networks, Tampa, FL, USA, 16–18 November 2004; pp. 455–462.

30. Gaffney, B. Considerations and Challenges in Real Time Locating Systems Design. White Paper. Available online: https://www.decawave.com/considerations-and-challenges-in-real-time-locating-systems-design/ (accessed on 16 April 2020).

31. Charlier, M.; Quoitin, B.; Bette, S.; Eliasson, J. Support for IEEE 802.15. 4 ultra wideband communications in the Contiki operating system. In Proceedings of the 2016 Symposium on Communications and Vehicular Technologies (SCVT), Mons, Belgium, 22 November 2016; pp. 1–6.

32. Zhang, Z.; Chu, D.; Chen, X.; Moscibroda, T. Swordfight: Enabling a new class of phone-to-phone action games on commodity phones. In Proceedings of the 10th International Conference on Mobile Systems, Applications, and Services, Low Wood Bay, UK, 25–29 June 2012; pp. 1–14.

33. Heinzelman, W.R.; Chandrakasan, A.; Balakrishnan, H. Energy-efficient communication protocol for wireless microsensor networks. In Proceedings of the 33rd Annual Hawaii International Conference on System Sciences, Maui, HI, USA, 4–7 January 2000; 10p.